



ORIGINAL ARTICLE

Experimental analysis and thermodynamic modelling of Nitroxynil solubility in pure solvent and binary solvent



Yang Chen¹, Nanxin Li¹, Jinping Lan¹, Xiaojuan Li, Wei Zhang, Funeng Xu, Haohuan Li, Gang Shu, Juchun Lin, Guangneng Peng, Huaqiao Tang, Ling Zhao, Hualin Fu*

Department of Pharmacy, College of Veterinary Medicine, Sichuan Agricultural University, Chengdu, Sichuan 611130, People's Republic of China

Received 8 April 2022; accepted 15 December 2022
Available online 29 December 2022

KEYWORDS

Nitroxynil;
Solubility;
Hansen solubility parameters (HSPs);
Activity coefficient;
Dissolution thermodynamics

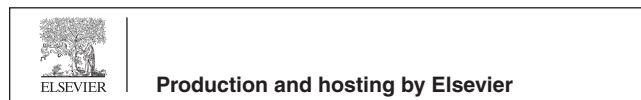
Abstract Nitroxynil(NIT) is a commonly used anti-liver fluke drug for cattle and sheep, Its solubility is closely related to its preparation. In this work, the molar solubility of NIT in nine pure solvents (methanol, ethanol, 1,2-propanediolethyl, isopropanol, ethyl acetate, acetonitrile, *n*-butanol, phemethylol) and two kinds of binary mixtures with different ratio(ethanol + phemethylol; ethanol + acetonitrile) was determined by shake flask method over the temperature from 278.15 ~ 323.15 K at atmosphere pressure. Results show that the solubility of NIT in all tested solvents was increased with raised temperature. In mono-solvents, the mole fraction solubility of NIT was highest in phemethylol and the solubility order is: phemethylol > acetonitrile > ethyl acetate > methanol > *n*-butanol > ethanol > 1,2-propanediolethyl > isopropanol > water. In binary solvents, the mole fraction solubility increased with increasing ratio of phemethylol/acetonitrile. In mono-solvents, the modified Apelblat equation, λ h equation, Van't Hoff model were applied to correlate the solubility data. In binary solvents, the modified Apelblat equation, λ h equation, GSM model and Jouyban-Acree model were to correlate the solubility data. Solubility order of NIT in nine pure solvent and two binary solvent systems were analysed by using the Hansen solubility parameter (HSP). Activity coefficient was to access the solute-solvent molecular interactions. In addition, the dissolution of NIT is an endothermic and entropy-friendly process, since thermodynamic parameters such as enthalpy, entropy, and apparent standard Gibbs free energy

* Corresponding author.

E-mail address: fuhl2005@sohu.com (H. Fu).

¹ These authors contributed equally to this work.

Peer review under responsibility of King Saud University.



are all greater than zero. The results will supply some essential data on recrystallization process, purification and formulation development of NIT in pharmaceutical applications.

© 2022 Published by Elsevier B.V. on behalf of King Saud University. This is an open access article under the CC BY-NC-ND license (<http://creativecommons.org/licenses/by-nc-nd/4.0/>).

1. Introduction

Solubility is a physical property that shows the thermodynamic balance of active pharmaceutical ingredients in solid–liquid mixtures. Among all the parameters during crystallization process, solid–liquid equilibrium data is of great importance to contribute to the design and optimization of purification processes (Akay et al., 2021). It should be noted that according to FDA, solubility and permeability are the sole critical factors in determining generic bioequivalence (Rezaei et al., 2021). Thus, the determination of solubility of drugs in different cosolvent media is significant, which can supply some reference for future developments.

Nitroxylin (NIT) is an anthelmintic veterinary drug; Its chemical name is 4-hydroxy-3-iodo-5-nitrobenzotrile (molecular formula: $C_7H_3IN_2O_3$; molar mass: $290.01 \text{ g}\cdot\text{mol}^{-1}$ and CASRN:1689–89–0; Figure. S1), which has been found as a yellow crystalline powder, almost odorless, slightly soluble in water, soluble in ethanol, ether and other organic solvents (Soliman et al., 2021). Corbett et al. (Corbett and Goose, 1971) studied the effect of NIT on mitochondrial function of mice liver cells, and proved that it is a kind of uncoupling agent for oxidative phosphorylation, it leads to death by blocking oxidative phosphorylation, reducing ATP concentration and reducing the energy required for cell division. A drug can only perform its pharmacological effects if it binds to a specific receptor, so it must exist in dissolved form before it can cross the gut barrier. This means that only soluble drugs can be used in the absorption process (Azarmi et al., 2007). Therefore, the solubility of drugs is closely related to the absorption of drugs in living organisms. To some extent, only understanding the solubility of a drug in a solvent can make it more effective. So far, the experimental solubility data of NIT in various kinds of solvent have not been systematically researched. Therefore, it is necessary to systematically measure the solubility of NIT in different solvent systems and predict solubility behavior using thermodynamic models. Besides, The single solvent we selected is a common solvent in pharmaceutical process, and the choice of binary solvent also provides a theoretical basis for the recrystallization and purification of NIT.

The main objectives of the study are to determine the solubility of NIT in nine pure solvents (methanol, ethanol, 1,2-propanediolethyl, isopropanol, ethyl acetate, acetonitrile, *n*-butanol, phemethylol) and two kinds of binary mixtures with different ratio (ethanol + phemethylol; ethanol + acetonitrile) at temperatures ranging from 278.15 K to 323.15 K under atmospheric pressure ($p = 0.1 \text{ MPa}$). Afterwards, experimental solubility results were correlated by different solubility models, the modified Apelblat model, the λh model, Van't Hoff model, GSM equation and Jouyban-Acree model (Li et al., 2017). Based on the concept of linear solvation energy relationship, Hansen solubility parameters (HSPs) were calculated to investigate the effect of solvents on the solid–liquid equilibrium process of NIT. Furthermore, the thermodynamic properties in dissolution, that is, the change of enthalpy (ΔH_{sol}^0), entropy (ΔS_{sol}^0) and Gibbs free energy (ΔG_{sol}^0), were calculated (Shekaari et al., 2018). The solubility data, solubility parameters and other physico-chemical parameters of NIT obtained in this research could be useful in purification, recrystallization, drug discovery, pre-formulation studies and formulation on development of NIT, especially in liquid dosage forms. (Alshehri and Shakeel, 2020).

2. Materials and methods

2.1. Materials

Nitroxinil was purchased from Huana Chemicals Co., Ltd. The more information of the solvents used in this study was presented in Table S1.

2.2. Experimental procedure for solubility determination

The solubility measurement method was similar to our previous literature (Chen et al., 2020). In this paper, the solubility of NIT was determined by gravimetric analysis in mono solvents and binary solvent mixtures. NIT concentrations were determined after appropriate gravimetric dilution with pure acetonitrile by measuring the UV light absorbance at the wavelength of second largest absorbance, 400 nm UV/visible spectrophotometry, followed by interpolation from a previously constructed UV spectrophotometric gravimetric calibration curve (Osorio et al., 2020). In order to obtain an accurate solubility, the reported solubility data is the averages of at least three measurements. The mole fraction solubility (x) of NIT can be obtained by the Eq. (1).

$$x = \frac{m_1/M_1}{m_1/M_1 + \sum (m_i/M_i)} \quad (1)$$

where m_1 and m_i stand for the mass of solute and the solvents, respectively. M_1 and M_i represent the molar mass of solute and the solvents, respectively.

2.3. Characterization methods

Differential scanning calorimetry (DSC) and powder X-ray diffractometry (PXRD) were used to characterize NIT in solid phases. DSC measurement was carried out by DSC-200F Instrument (NETZSCH Scientific Instruments Trading (Shanghai) Ltd., Germany). Sapphire was selected as the reference. 6.05 mg NIT was put into a alumina pan and measured in the range of 293.15 K to 473.15 K at heating rate of $10 \text{ K}\cdot\text{min}^{-1}$ under a N_2 atmosphere ($100 \text{ mL}\cdot\text{min}^{-1}$). PXRD analysis of raw and equilibrated NIT was performed using DX-2800 Diffractometer (Haoyuan Instrument Co., Ltd., China). The 2θ range for recording these spectra was set at $2\text{--}70^\circ$ with a scan speed of $3.0^\circ \text{ min}^{-1}$ (Wei et al., 2021).

2.4. Hansen solubility parameters (HSPs)

Hansen dissolvability coefficient was employed in this study to clarify the dissolution characteristics of solid in the solvents. The overall HSP (δ_t) is determined as Eq (2): (Yang et al., 2019) (Brett, 2007)

$$\delta_t = \sqrt{\delta_d^2 + \delta_p^2 + \delta_h^2} \quad (2)$$

Where δ_d , δ_p and δ_h separately denote dispersion, polar and hydrogen bonded coefficients for Hansen dissolvability. The total and partial Hansen solubility parameters for NIT are estimated by way of group contribution method proposed by Hoftyzer and van Krevelen as Eq (3)-(5) (Shen et al., 2021) (Liu et al., 2021) (Mohammad et al., 2011)

$$\delta_d = \frac{\sum F_{di}}{V} \quad (3)$$

$$\delta_p = \frac{\sqrt{\sum F_{pi}^2}}{V} \quad (4)$$

$$\delta_h = \frac{\sqrt{\sum E_{hi}}}{V} \quad (5)$$

where the F_{di} and F_{pi} represent dispersion force and polarity force of each structure groups i , respectively. The E_{hi} represents hydrogen bond interaction energy. V is the group contribution to the molar volume of solute. For NIT, the values of F_{di} , F_{pi} and E_{hi} for group contribution method calculation of NIT are given in Table S2.

The HSPs of commonly used solvents can be found in many published literatures, while the HSPs for selected binary solvents mixture (δ_M^{mix}) can be calculated by Eq.(6)(Li et al., 2021)

$$\delta_M^{mix} = \alpha\delta_M^1 + (1 - \alpha)\delta_M^2 \text{ for } M = d, p \text{ and } h \quad (6)$$

Herein, the superscript of 1 and 2 represent the solvent ethanol and (phenethylol, acetonitrile) respectively, and α represents the volume fraction of positive solvent 1 in the binary solvents mixture. The HSPs (δ_t , δ_d , δ_p and δ_h) of the selected two binary solvents as listed in Tables S3.

The Bagley diagram with a two-dimensional plot of the volume-dependent solubility parameter δ_v against δ_H has been used in the miscibility investigations and predictions the duration of intestinal absorption for various drugs, δ_v can be described as Eq.(7)

$$\delta_v = \sqrt{\delta_d^2 + \delta_p^2} \quad (7)$$

and subsequently the $R_{a(v)}$ factor was used to determine the miscibility as Eq.(8)

$$R_{a(v)} = \sqrt{4(\delta_v2 - \delta_v1)^2 + (\delta_h2 - \delta_h1)^2} \quad (8)$$

R_a can be employed to show the miscibility/solubility between solvent and solute. If the solute has better solubility, the R_a magnitude should be $< 5.6 \text{ MPa}^{1/2}$. So one may estimate the solvent property for solute solubility in terms of the R_a value. The higher the R_a value is, the poor solute solubility will be. The case is vice versa. As a result, the magnitude of $R_a < 5.6 \text{ MPa}^{1/2}$ is suggested for better solubility of a solute (Huang et al., 2021)(Mohammad et al., 2011).

Recently, the difference of total solubility parameters ($\Delta\delta_t$ and $\Delta\delta$) between the solute and solvent has been used as a tool to predict miscibility as Eq.(9)-(10)(Li et al., 2021):

$$\Delta\delta_t = |\delta_t2 - \delta_t1| \quad (9)$$

$$\Delta\delta = \sqrt{(\delta_h2 - \delta_h1)^2 + (\delta_p2 - \delta_p1)^2 + (\delta_d2 - \delta_d1)^2} \quad (10)$$

where the subscript of 1 and 2 represents the solute and the solvent, respectively, and the variables (δ_t , δ_d , δ_p and δ_h) have the same definition as that in the previous equations, and suggested a general trend indicating that materials with $\Delta\delta_t < 7 \text{ MPa}^{0.5}$ are miscible, while with $\Delta\delta_t$ greater than $7 \text{ MPa}^{0.5}$ are immiscible. (Greenhalgh et al., 1999).

The HSPs (δ_t , δ_d , δ_p and δ_h) of the selected nine pure solvents can be obtained directly from the literatures (Huang et al., 2021) (Zhang et al., 2021) (Sha et al., 2021a) (Cao et al., 2020), which was listed in Tables S3.

3. Solid-liquid equilibrium models

The solubility data of NIT in different pure solvents and mixture solvents were correlated by various thermodynamic models, such as the modified Apelblat equation, λh equation, Jouyban-Acree equation, GSM equation were employed to correlate the NIT solubility in different solvents.

3.1. Modified Apelblat model

The modified Apelblat model has already been one of the most commonly and widely used models in solubility correlation and prediction, especially in engineering applications. This model can give the variation trend of solubility with temperature in the same proportion of solvent, and the correlation with the three parameters is relatively accurate (Shen et al., 2021) (Liu et al., 2021):

$$\ln x = \frac{a}{T(\text{K})} + b + c \ln(T(\text{K})) \quad (11)$$

Where a , b and c are the empirical parameters, a and b have the same meaning as in the modified Apelblat model, the value of c represents the effect of temperature on the fusion enthalpy.

3.2. λh model

The λh equation is a semi-empirical model and can be used to correlate the experimental solubility data for the solid-liquid equilibrium systems (Jia et al., 2021),

$$\ln \left[1 + \frac{\lambda(1-x)}{x} \right] = \lambda h \left[\frac{1}{T(\text{K})} - \frac{1}{T_m(\text{K})} \right] \quad (12)$$

Where x is the mole fraction of NIT in different solutions, T stands for the absolute temperature and T_m is the standard melting point of Kelvin temperature. λ and h are determined by correlation of solubility data.

3.3. GSM model

GSM equation was used to calculate the solubility in binary solvents which is one of the theoretical models (Chen et al., 2020), The model is presented as Eq. (13)

$$\ln x = a + bx_j^0 + c(x_j^0)^2 + d(x_j^0)^3 + e(x_j^0)^4 \quad (13)$$

Where a , b , c , d and e were the model's five parameters, x_j^0 refers to the initial mole fraction of ethanol under the assumption of solute is not present.

3.4. Jouyban-Acree model

The Jouyban-Acree model is suggested to describe the solubility of a solute with the variation of both temperature and initial composition of binary solvent mixtures (Yang et al., 2021). The model was presented as Eq. (14)

$$\ln x_T = x_j^0 \ln(x_j)_T + x_i^0 \ln(x_i)_T + x_j^0 x_i^0 \times \sum_{i=0}^n J_i (x_j^0 - x_i^0)^i / T(K) \quad (14)$$

where x_T , $(x_j)_T$ and $(x_i)_T$ are the mole fraction solubility of solute in solvent mixture or pure solvent (j or i) of mixture composition at the same experimental temperature (T) respectively, and J_i is the model constant.

In GSM Eq. (13), $(x_j)_T$ and $(x_i)_T$ can be obtained based on Van't Hoff in the above. When $n = 2$, a new equation (15) which called Van't-JA model can be obtained.

$$\ln x_T = x_j^0 (a_j + b_j / T(K)) + x_i^0 (a_i + b_i / T(K)) + \frac{x_j^0 x_i^0 \left[J_0 + J_1 (x_j^0 - x_i^0) + J_2 (x_j^0 - x_i^0)^2 \right]}{T(K)} \quad (15)$$

Introducing constant parameters (V_0 to V_6) to Eq. (15), it can be further simplified as Eq. (16).

$$\ln x = V_0 + \frac{V_1}{T(K)} + V_2 x_j^0 + \frac{\left[V_3 x_j^0 + V_4 (x_j^0)^2 + V_5 (x_j^0)^3 + V_6 (x_j^0)^4 \right]}{T(K)} \quad (16)$$

3.5. Evaluation of thermodynamic models

In order to evaluate the applicability of the tested models, the root-mean-square deviations (RMSD) were calculated as follows equation (17) (R. Sun et al., 2021).

$$RMSD = \sqrt{\frac{\sum_{i=1}^N (x^{\text{exp}} - x^{\text{cal}})^2}{N}} \quad (17)$$

Where N refers the number of experimental data points, x^{exp} and x^{cal} denote the experimental data and model predicted data, respectively.

4. Results and discussion

4.1. Characterization of NIT in solid phases

The solid phases of pure and equilibrated NIT were characterized using DSC and PXRD techniques. The representative DSC spectra of pure NIT is presented in Figure S2. It can be seen that there is a sharp exothermic peak at 402.62 K, which indicates the melting temperature of NIT is 402.62 K and the fusion enthalpy ($\Delta_{\text{fus}}H$) is calculated to be 42.75 kJ/mol (Alanazi et al., 2020). At present, no literatures have reported the T_m value and $\Delta_{\text{fus}}H$ of NIT. The differences of sample sources, measurement methods and environments (such as heating rates), purity and purification method may be the factor resulting in slight deviations of melting point and fusion

enthalpy between experiment value and literature data (Huang et al., 2021).

The crystalline state for raw material and samples gained from the solution of NIT after dissolution equilibrium were tested by the XRPD and were depicted in Figure S3. From Figure S3, it can be found that no new characteristic peaks were observed, which suggested that no crystal form transition occurred during the dissolution process of NIT in all pure solvents studied. Note that the minor differences among PXRD patterns in peak intensity is likely due to the preferred orientation of samples (Asadi et al., 2020) (Jouyban et al., 2020).

4.1.1. In pure solvents

The studied organic solvents consist of an ester solvent, a nitrile compound and six alcohol solvents. It is obvious that the maximum solubility is in phemethylol and the solubility order in pure solvents is: phemethylol > acetonitrile > ethyl acetate > methanol > n-butanol > ethanol > 1,2-propanediolethyl > isopropanol > water, whose sequence was not completely consistent with the polar sequence of solvents (water > methanol > ethanol > phemethylol > n-butanol > isopropanol > acetonitrile > ethyl acetate). The experimental data indicates that the "like dissolves like" rule is not the only factor to determine the solubility of NIT. It is known to all that the solubility of solute was not only influenced by polarity of the solvent, but decided by the size of molecular, spatial conformation, solvent-solute interaction and other factors. The solubility is the result of the comprehensive influence of all factors (W. Sun et al., 2021).

The solubility values of NIT in the chosen mono-solvents of at temperature from 278.15 K to 323.15 K are listed in Table 1 and presented graphically in Figure 3. It can be seen clearly from the trend graph that the solubility of the compound increased with increasing temperature in nine pure solvents. The solubility of NIT in phemethylol, acetonitrile and ethyl acetate increased significantly with the increase of temperature, even a saturation trend was not reached at the test temperature; On the contrary, in methanol, n-butanol, ethanol, 1,2-propanediolethyl, isopropanol and water, the value did not increase significantly with the increase of temperature, but showed a gentle trend. Experimental data indicate that those with similar structures may be mutually soluble, phemethylol and NIT contain benzene rings, therefore, NIT has the highest solubility in phemethylol. Moreover, NIT and acetonitrile are nitrile compounds. The effect of structural similarity on the solubility of NIT was greater than that of polar similarity.

4.1.2. In binary solvent mixtures

According to the experimental results of 4.2.1, the solubility of NIT in phemethylol and acetonitrile are greater than that of other organic solvents. As we all known, the solubility is a function of temperature and components of solvent, therefore the solubility of NIT at various binary solvent mixtures (ethanol + phemethylol; ethanol + acetonitrile) increases not only with the rising temperature and also the rise of the ratio phemethylol/acetonitrile content at constant temperature, just as displayed in Tables. 2 and 3 and graphically shown in Figures 5 and 6. According to Figures 5 and 6, it can be seen that the solubility of NIT increased along with temperature in both investigated binary solvent mixtures, and the solubility was increased as the mole fraction of phemethylol/acetonitrile

Table 1 Experimental and calculated mole fraction solubility of NIT in nine mono-solvent systems from 278.15 K to 323.15 K ($p = 101.3$ kpa).^{a,b}

T/K	$10^3 x^{\text{exp}}$	$10^3 x^{\text{Apel}}$	$10^3 x^{\lambda h}$	$10^3 x^{\text{exp}}$	$10^3 x^{\text{Apel}}$	$10^3 x^{\lambda h}$
	water			methanol		
278.15	0.66	0.65	0.66	9.50	8.87	8.99
283.15	0.74	0.71	0.72	10.94	10.13	10.22
288.15	0.77	0.79	0.79	11.16	11.55	11.59
293.15	0.88	0.86	0.86	12.02	13.13	13.13
298.15	0.96	0.95	0.94	14.47	14.91	14.86
303.15	1.02	1.04	1.03	16.61	16.88	16.79
308.15	1.13	1.14	1.13	20.39	19.08	18.97
313.15	1.20	1.25	1.24	20.50	21.52	21.43
318.15	1.39	1.36	1.36	25.07	24.22	24.21
323.15	1.51	1.49	1.50	26.95	27.22	27.37
	ethanol			1,2-propanediolethyl		
278.15	7.48	7.22	7.38	6.86	6.14	6.64
283.15	8.12	8.1	8.2	7.45	6.96	7.40
288.15	9.46	9.07	9.1	8.60	7.87	8.24
293.15	10.11	10.13	10.1	8.83	8.89	9.17
298.15	10.97	11.29	11.21	10.21	10.01	10.21
303.15	12.19	12.56	12.44	10.96	11.25	11.36
308.15	14.10	13.94	13.82	12.35	12.62	12.64
313.15	14.85	15.44	15.35	14.47	14.13	14.09
318.15	17.22	17.08	17.08	15.55	15.79	15.71
323.15	19.24	18.86	19.04	17.75	17.62	17.54
	isopropanol			ethyl acetate		
278.15	5.17	5.14	5.24	79.35	79.69	77.55
283.15	6.09	5.78	5.85	85.91	91.48	90.15
288.15	6.83	6.49	6.52	99.12	104.74	104.24
293.15	7.52	7.27	7.26	118.80	119.64	119.90
298.15	7.86	8.13	8.08	142.41	136.35	137.24
303.15	8.48	9.07	9.00	162.33	155.04	156.34
308.15	9.65	10.10	10.02	179.60	175.92	177.31
313.15	11.06	11.23	11.17	196.90	199.19	200.23
318.15	12.93	12.47	12.46	224.39	225.09	225.17
323.15	13.97	13.81	13.93	250.88	253.85	252.23
	acetonitrile			<i>n</i> -butanol		
278.15	54.72	57.09	52.95	8.02	7.64	7.53
283.15	72.77	69.05	66.15	9.38	8.76	8.66
288.15	85.91	83.23	81.82	9.90	10.04	9.93
293.15	108.17	100.00	100.23	11.37	11.49	11.36
298.15	119.70	119.79	121.59	12.45	13.13	12.98
303.15	136.32	143.06	146.09	14.26	14.98	14.81
308.15	161.89	170.36	173.89	16.46	17.08	16.88
313.15	200.96	202.29	205.04	18.85	19.44	19.23
318.15	244.40	239.57	239.53	22.42	22.11	21.90
323.15	284.23	282.96	277.25	25.29	25.11	24.95
	phemethylol					
278.15	78.16	75.71	67.12			
283.15	84.33	91.77	85.40			
288.15	110.90	110.85	107.30			
293.15	125.32	133.46	133.12			
298.15	160.99	160.16	163.08			
303.15	199.27	191.60	197.24			
308.15	226.26	228.53	235.52			
313.15	285.49	271.79	277.66			
318.15	317.43	322.34	323.19			
323.15	376.96	381.24	371.52			

x^{Apel} , $x^{\lambda h}$ indicate the calculated mole fraction solubility of NIT obtained by the modified Apelblat model, λh model respectively.

^a x^{exp} refers to the experimental mole fraction solubility of NIT.

^b The relative standard deviation of the solubility measurement $u(x) = 0.001$, $u(T) = 0.05$ K, $u(P) = 2$ KPa.

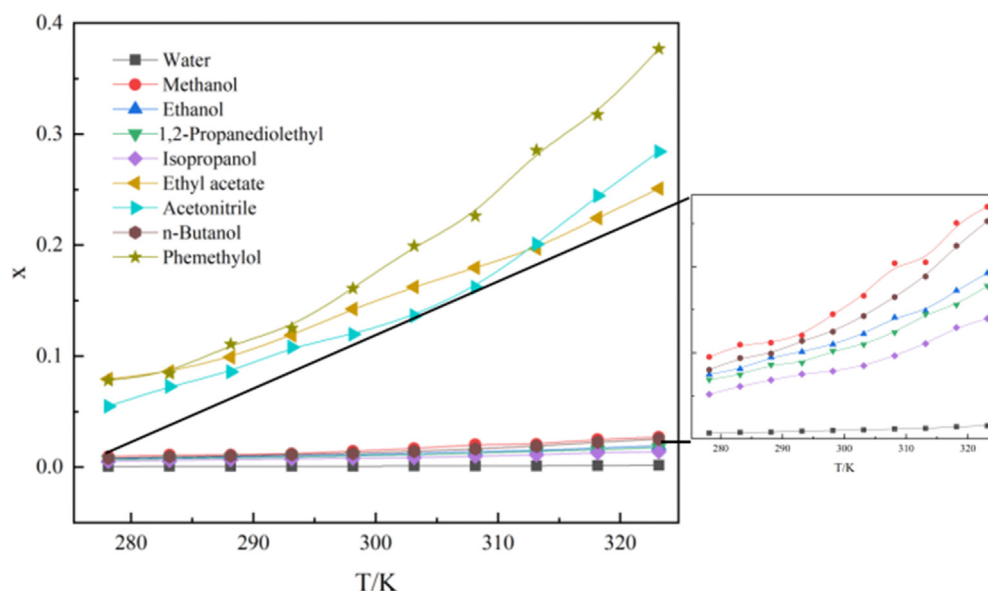


Fig. 1 Mole fraction solubility (x) of NIT in nine pure solvents.

increases. As long as phemethylol or acetonitrile was added into the binary solvent, the solubility of NIT showed an obvious increasing trend, indicating that phemethylol and acetonitrile can significantly increase the dissolution of NIT, and the greater the proportion of phemethylol and acetonitrile, the more obvious the dissolution ability.

There are many factors that affect the solubility and its changed trends. In addition to the interaction between the solvents, the interaction between the solute and the solvent, the properties of solvent and solute (such as dielectric constant, polarity, dipole moment, cohesive energy, ionization constant,

the surface tension etc.) and so on will also affect the solubility. The influencing factors are numerous and complex, and the specific reasons that affecting the solubility of NIT need to be further studied (Xue et al., 2021).

4.2. Solubility parameters for NIT and various organic solvents

Values of δ_d , δ_p , δ_h , $\Delta\delta_t$ and δ_v for NIT and selected mono-solvents are listed in Table S4, and values of F_{di} , F_{pi} and E_{hi} for group contribution method calculation of NIT are presented in Table S2. Total HSP (δ) for NIT was obtained as

Table 2 Experimental and calculated mole fraction solubility of NIT in binary mixed solvents of ethanol + phemethylol with different ratio within a temperature range from 278.15 K to 323.15 K ($p = 101.3$ kpa).^{a,b,c}.

T/K	$10^3 x_j^{\text{exp}}$	$10^3 x_j^{\text{ApeI}}$	$10^3 x_j^{\lambda h}$	$10^3 x_j^{\text{GSM}}$	$10^3 x_j^{\text{Van}'r\text{-JA}}$
$x_j^0 = 0.00$					
278.15	78.16	75.71	67.12	77.51	70.51
283.15	84.33	91.77	85.40	83.12	87.32
288.15	110.90	110.85	107.30	110.62	107.33
293.15	125.32	133.46	133.12	124.94	131.01
298.15	160.99	160.16	163.08	161.12	158.85
303.15	199.27	191.60	197.24	198.22	191.38
308.15	226.26	228.53	235.52	226.65	229.18
313.15	285.49	271.79	277.66	285.06	272.88
318.15	317.43	322.34	323.19	317.44	323.13
323.15	376.96	381.24	371.52	374.62	380.64
$x_j^0 = 0.10$					
278.15	64.22	67.27	61.50	64.22	64.72
283.15	77.06	80.90	76.72	80.74	79.31
288.15	105.87	96.97	94.71	106.91	96.49
293.15	110.99	115.86	115.71	112.22	116.62
298.15	132.72	138.01	139.94	131.91	140.05
303.15	161.87	163.91	167.54	165.82	167.18
308.15	197.56	194.12	198.56	195.76	198.41
313.15	229.06	229.27	232.99	231.29	234.20
318.15	289.44	270.05	270.69	290.07	275.01

Table 2 (continued)

T/K	$10^3 \cdot x^{\text{exp}}$	$10^3 \cdot x^{\text{Apel}}$	$10^3 \cdot x^{\text{zh}}$	$10^3 \cdot x^{\text{GSM}}$	$10^3 \cdot x^{\text{Van't-JA}}$
323.15	302.88	317.27	311.43	313.52	321.33
$x_j^0 = 0.20$					
278.15	56.69	56.79	52.76	56.58	57.64
283.15	76.05	68.67	65.87	73.23	69.92
288.15	93.36	82.76	81.43	91.54	84.25
293.15	99.00	99.43	99.69	97.32	100.87
298.15	109.27	119.09	120.88	110.71	120.04
303.15	141.83	142.21	145.20	137.47	142.03
308.15	161.14	169.33	172.78	162.92	167.14
313.15	195.20	201.06	203.69	189.30	195.67
318.15	247.20	238.10	237.93	243.19	227.94
323.15	282.20	281.23	275.39	264.33	264.28
$x_j^0 = 0.30$					
278.15	52.37	50.64	49.05	49.12	50.09
283.15	64.84	59.75	58.78	63.75	60.17
288.15	71.99	70.28	69.99	74.30	71.83
293.15	80.21	82.45	82.80	82.63	85.23
298.15	94.87	96.47	97.37	93.94	100.55
303.15	112.45	112.59	113.84	113.06	117.97
308.15	128.64	131.07	132.36	132.47	137.71
313.15	143.32	152.22	153.08	154.33	159.95
318.15	183.59	176.37	176.13	193.35	184.91
323.15	205.05	203.89	201.66	219.84	212.81
$x_j^0 = 0.40$					
278.15	41.34	41.06	39.81	43.20	42.59
283.15	49.37	53.86	48.37	54.24	50.69
288.15	58.77	62.21	58.37	59.81	59.97
293.15	69.75	72.15	69.95	69.23	70.55
298.15	82.55	76.83	83.28	79.52	82.53
303.15	97.43	91.05	98.53	92.12	96.06
308.15	114.68	114.25	115.88	106.10	111.25
313.15	134.62	136.50	135.50	124.04	128.25
318.15	157.64	159.20	157.56	149.29	147.18
323.15	184.14	184.47	182.23	177.68	168.19
$x_j^0 = 0.50$					
278.15	38.70	36.59	36.29	38.16	35.44
283.15	44.12	42.63	42.57	45.48	41.81
288.15	47.98	49.55	49.71	48.89	49.04
293.15	57.95	57.43	57.79	57.30	57.22
298.15	74.10	66.40	66.92	66.29	66.40
303.15	76.94	76.60	77.22	74.10	76.69
308.15	82.78	88.15	88.80	83.94	88.16
313.15	93.89	101.22	101.80	97.50	100.89
318.15	113.20	115.98	116.40	113.20	114.97
323.15	141.75	132.62	132.75	138.29	130.49
$x_j^0 = 0.60$					
278.15	32.34	33.58	30.49	33.30	28.80
283.15	36.70	36.05	34.48	37.54	33.69
288.15	40.36	39.14	38.89	40.62	39.19
293.15	43.60	42.96	43.79	46.60	45.36
298.15	46.91	47.61	49.24	53.72	52.24
303.15	52.88	53.25	55.28	58.50	59.89
308.15	59.60	60.07	62.02	65.42	68.36
313.15	68.32	68.31	69.52	74.52	77.69
318.15	78.46	78.24	77.91	85.55	87.95
323.15	90.30	90.23	87.31	103.33	99.17
$x_j^0 = 0.70$					
278.15	26.82	24.22	24.34	28.00	22.72
283.15	30.23	27.86	28.00	30.16	26.37
288.15	32.72	31.98	32.11	33.61	30.44
293.15	35.30	36.63	36.73	36.82	34.98
298.15	41.05	41.86	41.92	41.80	40.00
303.15	46.44	47.75	47.74	44.94	45.54

(continued on next page)

Table 2 (continued)

T/K	$10^3 x^{\text{exp}}$	$10^3 x^{\text{Apel}}$	$10^3 x^{\lambda h}$	$10^3 x^{\text{GSM}}$	$10^3 x^{\text{Van't-JA}}$
308.15	52.07	54.35	54.28	49.81	51.63
313.15	59.78	61.75	61.63	55.21	58.30
318.15	69.61	70.03	69.91	63.55	65.58
323.15	82.64	79.28	79.26	74.34	73.50
$x_j^0 = 0.80$					
278.15	23.79	23.27	23.77	21.95	17.28
283.15	25.11	25.28	25.55	23.10	19.90
288.15	27.34	27.43	27.48	26.51	22.82
293.15	30.71	29.72	29.57	27.74	26.04
298.15	32.41	32.16	31.87	30.86	29.58
303.15	34.22	34.75	34.38	33.24	33.46
308.15	36.73	37.51	37.15	36.56	37.70
313.15	39.34	40.44	40.21	39.59	42.32
318.15	42.58	43.55	43.62	45.93	47.33
323.15	48.81	46.85	47.43	51.95	52.75
$x_j^0 = 0.90$					
278.15	16.48	15.65	15.91	15.38	12.52
283.15	18.25	17.56	17.73	16.37	14.33
288.15	19.56	19.67	19.74	18.70	16.33
293.15	20.94	21.98	21.95	19.46	18.52
298.15	24.58	24.53	24.40	21.35	20.92
303.15	27.34	27.31	27.13	23.37	23.53
308.15	29.88	30.37	30.16	25.36	26.37
313.15	33.07	33.70	33.54	27.52	29.45
318.15	37.39	37.34	37.34	31.57	32.76
323.15	42.08	41.31	41.61	35.79	36.34
$x_j^0 = 1.00$					
278.15	7.48	7.22	7.38	9.18	8.53
283.15	8.12	8.10	8.20	10.31	9.72
288.15	9.46	9.07	9.10	10.80	11.01
293.15	10.11	10.13	10.10	12.31	12.43
298.15	10.97	11.29	11.21	13.69	13.97
303.15	12.19	12.56	12.44	15.38	15.64
308.15	14.10	13.94	13.82	16.23	17.45
313.15	14.85	15.44	15.35	18.61	19.40
318.15	17.22	17.08	17.08	19.98	21.50
323.15	19.24	18.86	19.04	24.82	23.74

^a x^{exp} is the experimental mole fraction solubility of NIT. x^{Apel} , $x^{\lambda h}$, $x^{\text{Van't-JA}}$ and x^{GSM} indicate the calculated mole fraction solubility of NIT obtained by the modified Apelblat model, λh model, Van't-JA model, GSM model respectively.

^b x_j^0 represents the initial mole fraction of ethanol in (ethanol + phemethylol) binary solvent system.

^c The relative standard deviation of the solubility measurement $u(x) = 0.001$, $u(T) = 0.05$ K, $u(P) = 2$ KPa.

24.94 MPa^{1/2}, indicating that NIT had lower polarity. It has been reported that the solvents having $R_{a(v)} < 5.6$ MPa^{0.5} are the most suitable for miscibility/solubility of solutes (Alanazi et al., 2020). From Table S3, values of $R_{a(v)}$ between NIT and all solvents are greater than 5.6 MPa^{0.5}, which means that NIT may be not soluble in all solvents. It has been reported that the solvents having $\Delta\delta_t < 7.0$ MPa^{0.5} are the most suitable for miscibility/solubility of solutes. (Alanazi et al., 2020) Except water and ethyl acetate all the investigated organic solvents had $\Delta\delta_t < 7.0$ MPa^{0.5}.

In order to have a deeper illustration of the relationship between solubility sequence of NIT and the investigated binary solvents, HSPs of measured solvents and NIT including (δ_d , δ_p , δ_h , $\Delta\delta_t$, δ_t and δ_v) were summarized in Table S2. As can be seen in Table S2, the δ_h of selected binary solvent was very close to that of NIT, indicating that hydrogen bond might be the main interaction energy in NIT and selected binary-solvents. With

the increment of mass fraction (x_j^0) of ethanol, the $\Delta\delta_d$, $\Delta\delta_p$ and $\Delta\delta_h$ of NIT in ethanol + phemethylol increased, the $\Delta\delta_d$ and $\Delta\delta_p$ of NIT in ethanol + acetonitrile decreased, however, the $\Delta\delta_h$ of NIT in ethanol + acetonitrile system decreased sharply with the rising mass fraction (x_j^0) of ethanol, achieved the minimum at a mass fraction of ethanol being 0.6000, and then followed by a sharp increase. Furthermore, all values of $\Delta\delta_t$ in ethanol + phemethylol was lower than 5.0 MPa^{0.5}. the $\Delta\delta_t$ of NIT in all two selected binary solvents decreased.

4.3. Activity coefficient

The activity coefficient calculation aimed to evaluate the solute-solvent molecular interactions to determine the optimal solvent for the solubilization of NIT. The ideal solubility of NIT is calculated by equation(18)(Liu and Guo, 2021)

Table 3 Experimental and calculated mole fraction solubility of NIT in binary mixed solvents of ethanol + acetonitrile with different ratio within a temperature range from 278.15 K to 323.15 K ($p = 101.3$ kpa).^{a,b,c}.

T/K	$10^3 x^{\text{exp}}$	$10^3 x^{\text{ApeI}}$	$10^3 x^{\lambda h}$	$10^3 x^{\text{GSM}}$	$10^3 x^{\text{Van}^r\text{-JA}}$
$x_j^0 = 0.00$					
278.15	78.16	75.71	67.12	77.51	70.51
283.15	84.33	91.77	85.4	83.12	87.32
288.15	110.9	110.85	107.3	110.62	107.33
293.15	125.32	133.46	133.12	124.94	131.01
298.15	160.99	160.16	163.08	161.12	158.85
303.15	199.27	191.6	197.24	198.22	191.38
308.15	226.26	228.53	235.52	226.65	229.18
313.15	285.49	271.79	277.66	285.06	272.88
318.15	317.43	322.34	323.19	317.44	323.13
323.15	376.96	381.24	371.52	374.62	380.64
$x_j^0 = 0.10$					
278.15	64.22	67.27	61.5	64.22	64.72
283.15	77.06	80.9	76.72	80.74	79.31
288.15	105.87	96.97	94.71	106.91	96.49
293.15	110.99	115.86	115.71	112.22	116.62
298.15	132.72	138.01	139.94	131.91	140.05
303.15	161.87	163.91	167.54	165.82	167.18
308.15	197.56	194.12	198.56	195.76	198.41
313.15	229.06	229.27	232.99	231.29	234.2
318.15	289.44	270.05	270.69	290.07	275.01
323.15	302.88	317.27	311.43	313.52	321.33
$x_j^0 = 0.20$					
278.15	56.69	56.79	52.76	56.58	57.64
283.15	76.05	68.67	65.87	73.23	69.92
288.15	93.36	82.76	81.43	91.54	84.25
293.15	99	99.43	99.69	97.32	100.87
298.15	109.27	119.09	120.88	110.71	120.04
303.15	141.83	142.21	145.2	137.47	142.03
308.15	161.14	169.33	172.78	162.92	167.14
313.15	195.2	201.06	203.69	189.3	195.67
318.15	247.2	238.1	237.93	243.19	227.94
323.15	282.2	281.23	275.39	264.33	264.28
$x_j^0 = 0.30$					
278.15	52.37	50.64	49.05	49.12	50.09
283.15	64.84	59.75	58.78	63.75	60.17
288.15	71.99	70.28	69.99	74.3	71.83
293.15	80.21	82.45	82.8	82.63	85.23
298.15	94.87	96.47	97.37	93.94	100.55
303.15	112.45	112.59	113.84	113.06	117.97
308.15	128.64	131.07	132.36	132.47	137.71
313.15	143.32	152.22	153.08	154.33	159.95
318.15	183.59	176.37	176.13	193.35	184.91
323.15	205.05	203.89	201.66	219.84	212.81
$x_j^0 = 0.40$					
278.15	41.34	41.06	39.81	43.2	42.59
283.15	49.37	53.86	48.37	54.24	50.69
288.15	58.77	62.21	58.37	59.81	59.97
293.15	69.75	72.15	69.95	69.23	70.55
298.15	82.55	76.83	83.28	79.52	82.53
303.15	97.43	91.05	98.53	92.12	96.06
308.15	114.68	114.25	115.88	106.1	111.25
313.15	134.62	136.5	135.5	124.04	128.25
318.15	157.64	159.2	157.56	149.29	147.18
323.15	184.14	184.47	182.23	177.68	168.19
$x_j^0 = 0.50$					
278.15	38.7	36.59	36.29	38.16	35.44
283.15	44.12	42.63	42.57	45.48	41.81
288.15	47.98	49.55	49.71	48.89	49.04
293.15	57.95	57.43	57.79	57.3	57.22
298.15	74.1	66.4	66.92	66.29	66.4
303.15	76.94	76.6	77.22	74.1	76.69

(continued on next page)

Table 3 (continued)

T/K	$10^3 x^{\text{exp}}$	$10^3 x^{\text{Apel}}$	$10^3 x^{\lambda h}$	$10^3 x^{\text{GSM}}$	$10^3 x^{\text{Van}'r\text{-JA}}$
308.15	82.78	88.15	88.8	83.94	88.16
313.15	93.89	101.22	101.8	97.5	100.89
318.15	113.2	115.98	116.4	113.2	114.97
323.15	141.75	132.62	132.75	138.29	130.49
$x_j^0 = 0.60$					
278.15	32.34	33.58	30.49	33.3	28.8
283.15	36.7	36.05	34.48	37.54	33.69
288.15	40.36	39.14	38.89	40.62	39.19
293.15	43.6	42.96	43.79	46.6	45.36
298.15	46.91	47.61	49.24	53.72	52.24
303.15	52.88	53.25	55.28	58.5	59.89
308.15	59.6	60.07	62.02	65.42	68.36
313.15	68.32	68.31	69.52	74.52	77.69
318.15	78.46	78.24	77.91	85.55	87.95
323.15	90.3	90.23	87.31	103.33	99.17
$x_j^0 = 0.70$					
278.15	26.82	24.22	24.34	28	22.72
283.15	30.23	27.86	28	30.16	26.37
288.15	32.72	31.98	32.11	33.61	30.44
293.15	35.3	36.63	36.73	36.82	34.98
298.15	41.05	41.86	41.92	41.8	40
303.15	46.44	47.75	47.74	44.94	45.54
308.15	52.07	54.35	54.28	49.81	51.63
313.15	59.78	61.75	61.63	55.21	58.3
318.15	69.61	70.03	69.91	63.55	65.58
323.15	82.64	79.28	79.26	74.34	73.5
$x_j^0 = 0.80$					
278.15	23.79	23.27	23.77	21.95	17.28
283.15	25.11	25.28	25.55	23.1	19.9
288.15	27.34	27.43	27.48	26.51	22.82
293.15	30.71	29.72	29.57	27.74	26.04
298.15	32.41	32.16	31.87	30.86	29.58
303.15	34.22	34.75	34.38	33.24	33.46
308.15	36.73	37.51	37.15	36.56	37.7
313.15	39.34	40.44	40.21	39.59	42.32
318.15	42.58	43.55	43.62	45.93	47.33
323.15	48.81	46.85	47.43	51.95	52.75
$x_j^0 = 0.90$					
278.15	16.48	15.65	15.91	15.38	12.52
283.15	18.25	17.56	17.73	16.37	14.33
288.15	19.56	19.67	19.74	18.7	16.33
293.15	20.94	21.98	21.95	19.46	18.52
298.15	24.58	24.53	24.4	21.35	20.92
303.15	27.34	27.31	27.13	23.37	23.53
308.15	29.88	30.37	30.16	25.36	26.37
313.15	33.07	33.7	33.54	27.52	29.45
318.15	37.39	37.34	37.34	31.57	32.76
323.15	42.08	41.31	41.61	35.79	36.34
$x_j^0 = 1.00$					
278.15	7.48	7.22	7.38	9.18	8.53
283.15	8.12	8.1	8.2	10.31	9.72
288.15	9.46	9.07	9.1	10.8	11.01
293.15	10.11	10.13	10.1	12.31	12.43
298.15	10.97	11.29	11.21	13.69	13.97
303.15	12.19	12.56	12.44	15.38	15.64
308.15	14.1	13.94	13.82	16.23	17.45
313.15	14.85	15.44	15.35	18.61	19.4
318.15	17.22	17.08	17.08	19.98	21.5
323.15	19.24	18.86	19.04	24.82	23.74

^a x^{exp} is the experimental mole fraction solubility of NIT. x^{Apel} , $x^{\lambda h}$, $x^{\text{Van}'r\text{-JA}}$ and x^{GSM} indicate the calculated mole fraction solubility of NIT obtained by the modified Apelblat model, λh model, Van' r -JA model, GSM model respectively.

^b x_j^0 represents the initial mole fraction of ethanol in (ethanol + acetonitrile) binary solvent system.

^c The relative standard deviation of the solubility measurement $u(x) = 0.001$, $u(T) = 0.05$ K, $u(P) = 2$ KPa.

Table 4 Thermodynamic parameters of NIT dissolution in nine pure solvents.^a

Solvent	ΔH_{sol}^0	ΔS_{sol}^0	ΔG_{sol}^0	ξ_{H}	ξ_{S}
	(KJ·mol ⁻¹)	(J·mol ⁻¹ ·K ⁻¹)	(KJ·mol ⁻¹)		
Water	13.56	-12.32	17.25	0.7858	0.2142
Methanol	18.03	25.61	10.35	0.7012	0.2988
Ethanol	15.49	14.75	11.06	0.7778	0.2222
1,2-Propanediolethyl	15.71	14.73	11.29	0.7806	0.2194
Isopropanol	15.78	13.00	11.88	0.8017	0.1983
Ethyl acetate	19.87	50.09	4.84	0.5694	0.4306
Acetonitrile	26.20	70.36	5.09	0.5538	0.4462
<i>n</i> -Butanol	18.87	27.35	10.67	0.6970	0.3030
Phemethylol	27.33	76.49	4.39	0.5436	0.4564

^a ΔH_{sol}^0 , ΔS_{sol}^0 and ΔG_{sol}^0 are the enthalpy, entropy and Gibbs energy of the solute, respectively. ξ_{H} and ξ_{S} are the contribution of enthalpy and entropy to the standard Gibbs energy, respectively.

Table 5 Thermodynamic parameters of NIT dissolution in binary solvent mixture of ethanol + phemethylol with different ratio.^{a,b}

x_j^0	ΔH_{sol}^0	ΔS_{sol}^0	ΔG_{sol}^0	ξ_{H}	ξ_{S}
	(KJ·mol ⁻¹)	(J·mol ⁻¹ ·K ⁻¹)	(KJ·mol ⁻¹)		
0.00	27.33	76.49	4.39	0.5436	0.4564
0.10	26.31	71.82	4.77	0.5498	0.4502
0.20	25.44	67.82	5.09	0.5556	0.4444
0.30	22.25	55.36	5.65	0.5727	0.4273
0.40	24.07	60.14	6.03	0.5716	0.4284
0.50	20.58	46.66	6.59	0.5953	0.4047
0.60	16.47	30.34	7.36	0.6440	0.3560
0.70	18.28	35.12	7.75	0.6344	0.3656
0.80	11.38	9.64	8.49	0.7973	0.2027
0.90	15.60	21.58	9.12	0.7067	0.2933

^a x_j^0 refers to the initial mole fraction of ethanol in the binary solvent.

^b ΔH_{sol}^0 , ΔS_{sol}^0 and ΔG_{sol}^0 are the enthalpy, entropy and Gibbs energy of the solute, respectively. ξ_{H} and ξ_{S} are the contribution of enthalpy and entropy to the standard Gibbs energy, respectively.

Table 6 Thermodynamic parameters of NIT dissolution in binary solvent mixture of ethanol + acetonitrile with different ratio.^{a,b}

x_j^0	ΔH_{sol}^0	ΔS_{sol}^0	ΔG_{sol}^0	ξ_{H}	ξ_{S}
	(KJ·mol ⁻¹)	(J·mol ⁻¹ ·K ⁻¹)	(KJ·mol ⁻¹)		
0.00	25.65	68.59	5.07	0.5549	0.4451
0.10	25.34	66.40	5.42	0.5599	0.4401
0.20	25.02	64.09	5.80	0.5655	0.4345
0.30	24.86	62.31	6.16	0.5708	0.4292
0.40	24.43	59.55	6.56	0.5776	0.4224
0.50	24.61	58.69	7.00	0.5830	0.4170
0.60	22.42	49.64	7.53	0.6009	0.3991
0.70	20.57	40.33	8.48	0.6297	0.3703
0.80	21.56	40.85	9.31	0.6377	0.3623
0.90	17.29	23.14	10.35	0.7136	0.2864

^a x_j^0 refers to the initial mole fraction of ethanol in the binary solvent.

^b ΔH_{sol}^0 , ΔS_{sol}^0 and ΔG_{sol}^0 are the enthalpy, entropy and Gibbs energy of the solute, respectively. ξ_{H} and ξ_{S} are the contribution of enthalpy and entropy to the standard Gibbs energy, respectively.

$$\ln x^{\text{idl}} = \frac{-\Delta_{\text{fus}}H(T_{\text{fus}} - T)}{RT_{\text{fus}}T} + \left(\frac{\Delta C_p}{R}\right) \left[\frac{T_{\text{fus}} - T}{T} + \ln\left(\frac{T}{T_{\text{fus}}}\right)\right] \quad (18)$$

Where R denotes the gas constant (8.314 J/K⁻¹·mol⁻¹); T_{fus} and $\Delta_{\text{fus}}H$ express fusion/melting temperature and fusion enthalpy of NIT, respectively, as achieved from DSC analysis; ΔC_p represents the difference in the molar heat capacity of the solid state from that of the liquid state. The ΔC_p was calculated by equation(19)

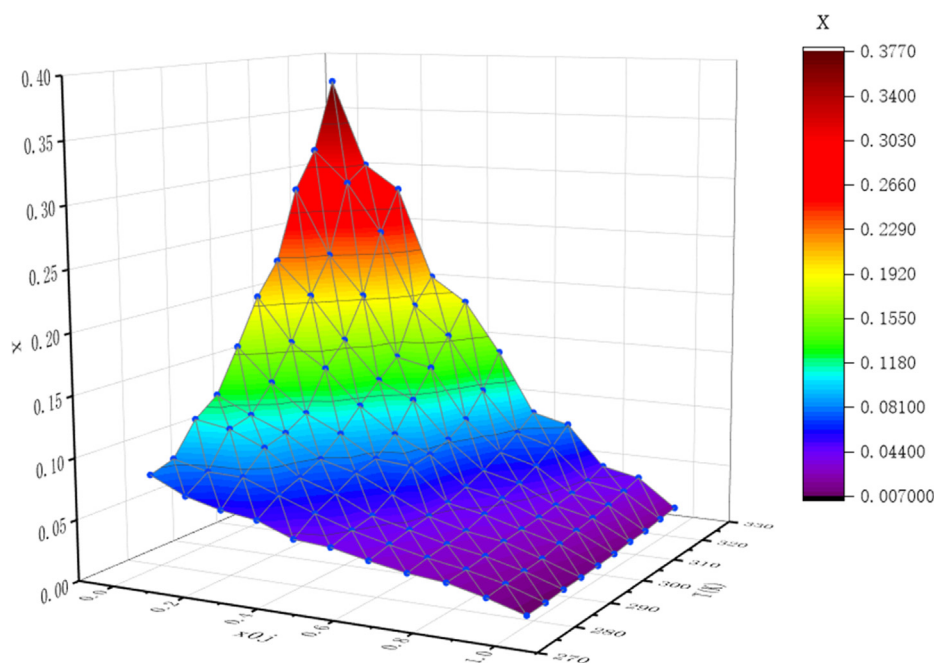


Fig. 2 Experimental solubility data of NIT at various temperatures $T(K)$ and different mole fraction compositions of acetone x_2^0 in the binary solvent mixtures of ethanol + phemethylol.

$$\Delta C_p = \frac{\Delta fus H}{T_{fus}} \quad (19)$$

The activity coefficient (γ_i) for NIT in different organic solvents was obtained by equation(20)

$$\gamma_i = \frac{x_i^{idl}}{x_i^{exp}} \quad (20)$$

where x_i^{idl} and x_i^{exp} are ideal solubility and experimental values.

Table S5-S7 summarizes the calculated values of γ_i for NIT in nine pure solvent and two binary solvent systems from T (278.15–323.15 K). γ_i in nine pure solvents satisfied the sequence of Phemethylol < Acetonitrile < Ethyl acetate < Methanol < *n*-Butanol < Ethanol < 1,2-Propanediolethyl < Iso-propanol < Water, which is opposed to the order of decreasing

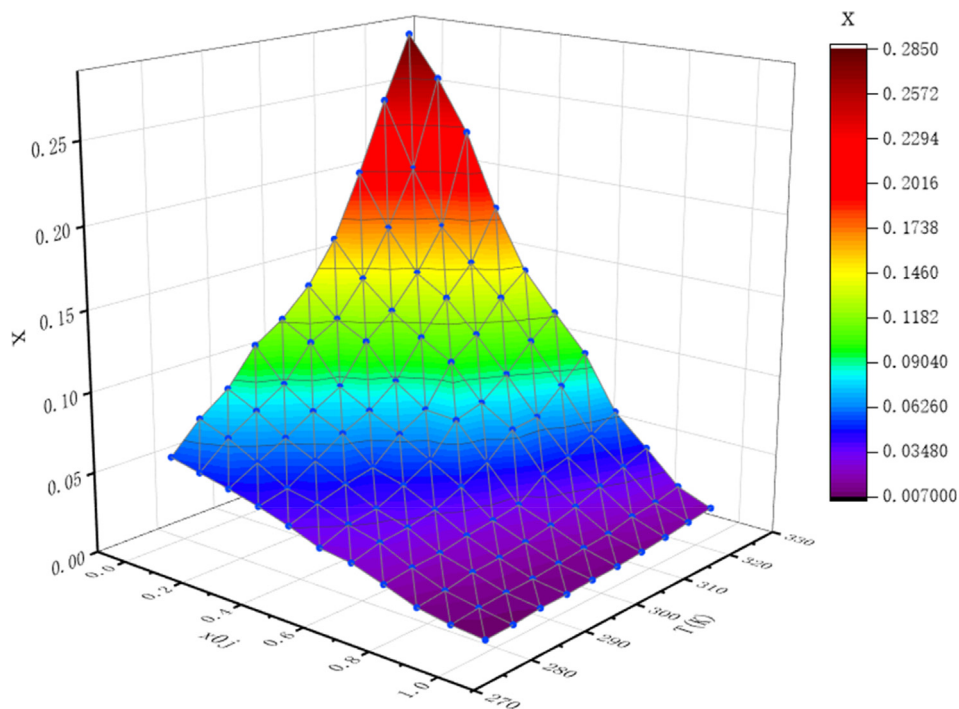


Fig. 3 Experimental solubility data of NIT at various temperatures $T(K)$ and different mole fraction compositions of acetone x_2^0 in the binary solvent mixtures of ethanol + acetonitrile.

solubility. The values of γ_i were recorded < 1.0 in organic solvents i.e., phemethylol, acetonitrile and ethyl acetate. Besides, the γ_i was decreased with the mole fraction of phemethylol/ acetonitrile increases in two binary solvent mixtures.

4.4. Comparison of model results

In this paper, the modified Apelblat model, λh model, GSM model and the Van't-JA model were used to fit the solubility of NIT in nine pure solvents and two binary mixed solvents.

As we can see from Tables 7-8, In pure solvent, both the modified Apelblat model and the λh model show a good fitting trend, the correlation coefficients (R^2) are above 0.98, the RMSD values are < 0.001 , the RMSD values of phemethylol, acetonitrile and ethyl acetate with good solubility were significantly higher than those of other solvents with poor solubility. it is worth noting that the modified Apelblat model(ORMSD = 1.9958×10^3) can give better correlation results though other models can also give satisfactory correlation results by used the 10^3 RMSD and 10^3 ORMSD values as appraisal standard in mono-solvents. From the theoretical values by the modified Apelblat model illustrated in Table 1, it can be found that the differences between the experimental and calculated values are very small.

As Tables 9-12 shown, the 10^3 RMSD and 10^3 ORMSD values of modified Apelblat model, λh model, Van't-JA model and GSM equation were calculated respectively, The correlation coefficients (R^2) were all greater than 0.7, and the fitting linearity was good. In modified Apelblat model, λh model

and Van't-JA model, the higher the ratio of phemethylol and acetonitrile, the higher the RMSD value, in GSM equation, RMSD value increased with the increase of temperature, which is similar to the result of the single solvent, It can be inferred that the stronger the solubility, the faster the solubility value increases, which will have an impact on the linear fitting. And the value of GSM model(ORMSD = 3.9109×10^3) is lowest in ethanol + phemethylol and Van't-JA model(RMSD = 4.41×10^3) is lowest in ethanol + acetonitrile. The results show that the GSM equation fits ethanol better, and ethanol + acetonitrile can be better fitted by Van't JA equation.

4.5. Apparent thermodynamics functions of dissolution

Thermodynamic properties are essential to the research of solid-liquid equilibrium systems, which can help us better understand the dissolution behavior of a drug. For the purpose of understand the dissolution process of NIT in the temperature range of 278.15 K–323.15 K, enthalpies of solution (ΔH_{sol}^0), Gibb's energy of dissolution (ΔG_{sol}^0) and entropy of solutions (ΔS_{sol}^0) have also been calculated by Van't Hoff plot from the intercept and slope.(Jia et al., 2021)(Yang et al., 2021).

$$\Delta H_{sol}^0 = -R \left[\frac{\partial \ln x}{\partial \left(\frac{1}{T} - \frac{1}{T_{mean}} \right)} \right] = -R \cdot slope \quad (21)$$

$$\Delta G_{sol}^0 = -RT_{mean} \cdot intercept \quad (22)$$

Table 7 Parameters of the Modified Apelblat equation for NIT in nine mono-solvents.^a

solvent	modified Apelblat model					
	a	b	c	R^2	10^3 RMSD	10^3 ORMSD
water	53.03	-39.85	5.74	0.9918	0.0243	1.9958
methanol	46.73	-47.85	7.63	0.9819	0.8233	
ethanol	-280.91	-34.70	5.47	0.9926	0.3172	
1,2-propanediolethyl	-261.20	-36.14	5.70	0.9908	0.3316	
isopropanol	-93.46	-40.30	6.28	0.9846	0.3428	
ethyl acetate	-62.64	-44.61	7.52	0.9943	4.2577	
acetonitrile	7.91	-63.12	10.70	0.9954	4.8693	
<i>n</i> -butanol	87.64	-52.14	8.34	0.9918	0.4982	
phemethylol	-75.71	-61.56	10.53	0.9956	6.4976	

^a a, b and c refer to the parameters of the modified Apelblat model.

Table 8 Parameters of the Van't Hoff model for NIT in nine mono-solvents.^a

solvent	λh model				
	λ	h	R^2	10^3 RMSD	10^3 ORMSD
water	0.01	840250.60	0.9944	0.0200	2.1026
methanol	0.05	32855.55	0.9821	0.7901	
ethanol	0.02	56588.44	0.9937	0.2569	
1,2-propanediolethyl	0.02	60099.83	0.9937	0.2749	
isopropanol	0.02	75751.85	0.9880	0.3029	
ethyl acetate	1.12	2141.11	0.9880	3.6055	
acetonitrile	3.19	1144.96	0.9911	6.7735	
<i>n</i> -butanol	0.06	33297.20	0.9933	0.4531	
phemethylol	6.44	629.54	0.9957	6.4464	

^a λ and h refer to the parameters of the λh model.

Table 9 Parameters of the modified Apelblat model for NIT in different ratio binary-solvents.^a

x_j^0	modified Apelblat model			R^2	10^3RMSD	10^3ORMSD
	a	b	c			
ethanol + phemethylol						
0.00	-280.91	-34.70	5.47	0.9956	6.4976	3.3570
0.10	-42.43	-59.96	10.20	0.9884	8.6838	
0.20	33.57	-63.66	10.78	0.9912	6.6963	
0.30	49.31	-56.36	9.45	0.9925	4.2191	
0.40	11.90	-59.52	10.00	0.9943	3.4297	
0.50	33.62	-52.39	8.70	0.9906	2.9556	
0.60	11614.42	-300.49	45.37	0.9985	0.6908	
0.70	207.11	-52.86	8.60	0.9876	1.9374	
0.80	62.07	-31.41	4.87	0.9855	0.9086	
0.90	16.02	-40.95	6.53	0.9948	0.5908	
1.00	-280.91	-34.70	5.47	0.9926	0.3172	
ethanol + acetonitrile						
0.00	7.91	-63.12	10.70	0.9954	4.8693	2.9990
0.10	58.03	-64.71	10.93	0.9896	6.3577	
0.20	71.50	-65.54	11.04	0.9843	6.7618	
0.30	17.62	-61.49	10.33	0.9970	2.4260	
0.40	-3875.64	26.40	-2.83	0.9895	3.7742	
0.50	23.39	-58.21	9.70	0.9912	2.8446	
0.60	150.83	-59.79	9.86	0.9890	2.4416	
0.70	226.65	-59.92	9.77	0.9805	2.1067	
0.80	9.45	-55.86	9.13	0.9929	0.5275	
0.90	77.79	-47.20	7.50	0.9900	0.5621	
1.00	-280.91	-34.70	5.47	0.9926	0.3172	

^a a, b and c refer to the parameters of the modified Apelblat model.

Table 10 Parameters of the λh model for NIT in different ratio binary-solvents.^a

x_j^0	λh model		R^2	10^3RMSD	10^3ORMSD
	λ	h			
ethanol + phemethylol					
0.00	6.44	629.54	0.9957	6.4464	3.8761
0.10	3.80	965.82	0.9895	8.2454	
0.20	3.14	11161.42	0.9852	8.6500	
0.30	1.21	2732.88	0.9898	4.9260	
0.40	1.26	2467.75	0.9922	4.0026	
0.50	0.52	4660.43	0.9736	5.0275	
0.60	0.17	9853.52	0.9883	1.9564	
0.70	0.21	9684.66	0.9882	1.8951	
0.80	0.02	28673.64	0.9899	0.7588	
0.90	0.05	24591.54	0.9966	0.4727	
1.00	0.02	56588.44	0.9952	0.2569	
ethanol + acetonitrile					
0.00	3.19	1144.96	0.9911	6.7735	3.5425
0.10	2.46	1439.67	0.9825	8.2570	
0.20	1.94	1790.47	0.9777	8.0578	
0.30	1.31	2455.99	0.9953	3.0505	
0.40	0.90	3316.02	0.9894	3.7884	
0.50	0.64	4384.81	0.9920	2.7070	
0.60	0.43	6155.71	0.9883	2.5154	
0.70	0.23	10433.87	0.9798	2.1414	
0.80	0.16	14744.23	0.9930	0.9137	
0.90	0.05	34743.54	0.9919	0.5063	
1.00	0.02	56588.44	0.9952	0.2569	

^a λ and h refer to the parameters of the λh model.

Table 11 Parameters of the GSM model for NIT in different ratio binary-solvents.^a

T/K	GSM model					R ²	10 ³ RMSD	10 ³ ORMSD	
	a	b	c	d	e				
ethanol + phemethylol									
278.15	-4.69	6.16	-10.92	10.32	-3.42	0.9937	1.6240	3.9109	
283.15	-4.57	5.37	-8.34	9.09	-4.03	0.9911	1.8154		
288.15	-4.53	6.83	-15.34	20.03	-9.20	0.9984	1.3355		
293.15	-4.40	5.21	-6.99	6.79	-2.69	0.9968	2.0535		
298.15	-4.29	0.86	-4.37	1.84	0.13	0.9939	3.5572		
303.15	-4.17	4.57	-4.18	3.14	-0.98	0.9970	3.1666		
308.15	-4.12	4.97	-5.53	5.50	-2.29	0.9969	3.8060		
313.15	-3.98	4.03	-1.10	-1.16	0.96	0.9944	6.3159		
318.15	-3.91	5.12	-6.16	7.69	-3.88	0.9967	5.7776		
323.15	-3.70	3.54	1.64	-4.96	2.49	0.9928	9.6574		
ethanol + acetonitrile									
278.15	-5.00	3.99	-1.81	-0.72	0.63	0.9970	0.8790		4.2904
283.15	-4.99	5.71	-7.36	5.85	-1.82	0.9958	1.3602		
288.15	-4.73	4.06	-2.86	1.49	-0.41	0.9991	24.1827		
293.15	-4.65	3.47	0.93	-4.84	2.86	0.9979	1.4197		
298.15	-4.71	5.38	-4.75	2.25	-0.28	0.9952	2.4877		
303.15	-4.59	4.85	-1.03	-3.76	2.54	0.9911	3.8989		
308.15	-4.41	4.62	1.02	-7.53	4.49	0.9984	1.9284		
313.15	-4.20	3.64	3.71	-10.36	5.61	0.9995	1.3448		
318.15	-4.17	4.98	-0.47	-5.48	3.73	0.9992	1.9917		
323.15	-4.18	7.67	-12.20	12.64	-5.18	0.9985	3.4107		

^a a,b,c,d and e refer to the parameters of the GSM model.

Table 12 Parameters of the Van't-JA model for NIT in different ratio binary-solvents.^a

x _j ⁰	Van't-JA model						R ²	10 ³ RMSD	
	V ₀	V ₁	V ₂	V ₃	V ₄	V ₅			V ₆
ethanol + phemethylol									
	2.58	-2043.70	6.87	-746.10	-1073.05	810.37	-315.37	0.9920	6.85
ethanol + acetonitrile									
	4.85	-2855.87	4.25	325.69	-991.31	-138.40	313.98	0.9944	4.41

^a V₀, V₁, V₂, V₃, V₄, V₅ and V₆ refer to the parameters of the Van't-JA model.

$$\Delta S_{sol}^0 = \frac{\Delta H_{sol}^0 - \Delta G_{sol}^0}{T_{mean}} \quad (23)$$

where R is the universal gas constant, T_{mean} represents the mean temperature and “intercept” is the intercept of ln x₁ and (1/T - 1/T_{mean}) curve.

Where T_{mean} represents the mean harmonic temperature of the temperature range which is given as Eq.(24).

$$T_{mean} = \frac{n}{\sum_{i=1}^n \frac{1}{T_i}} \quad (24)$$

Where n is the number of experimental temperatures points. In this work, the value of T_{mean} is 299.96 K.

The resulting data of ΔH_{sol}⁰, ΔG_{sol}⁰ and ΔS_{sol}⁰ for NIT dissolution are furnished in Table. 4-6. Besides, the contribution of enthalpy and entropy to the standard Gibbs energy also be calculated as Eq.(25), and shown in Table 4-6, too.

$$\xi_H = \frac{|\Delta H_{sol}^0|}{|\Delta H_{sol}^0| + |T_{mean} \cdot \Delta S_{sol}^0|} \quad (25)$$

$$\xi_S = \frac{|T_{mean} \cdot \Delta S_{sol}^0|}{|\Delta H_{sol}^0| + |T_{mean} \cdot \Delta S_{sol}^0|}$$

From Table. 4-6, In single solvent except water, the values of ΔS_{sol}⁰ were positive, which indicated the entropically driven dissolution process of NIT in the solvent. When NIT was dissolved in water, the degree of the system chaos is decreased, that is, the entropy of the system is decreased, so the ΔS_{sol}⁰ showed negative values. The conclusion can be drawn that ΔH_{sol}⁰ and ΔG_{sol}⁰ for NIT dissolution are positive in the studied mono and binary solvent mixtures, which explains the increasing solubility of NIT as the temperature increases. ΔG_{sol}⁰ > 0 indicating that the dissolution process of NIT is apparently not spontaneous. In addition, the higher the mole fraction solubility of NIT shows, the smaller the values of ΔG_{sol}⁰ are. It indicated that forming the force between solute and solvent needed less energy in the solvent system corresponding to the better dissolving performance, ΔH_{sol}⁰ > 0, which suggests that the dissolution process is endothermic(Wei et al., 2021). All of the ΔH_{sol}⁰ values are positive and the reason may be that the solute-solvent interaction force is less than other interactions (solute-solute and solvent-solvent interaction) in the dissolution process of NIT. Furthermore, ξ_H > ξ_S in both pure

and mixed solvent, which suggests ΔH_{sol}^0 is the main contributor to the standard molar Gibbs energy of solution during the dissolution and the values of ξ_{H} are $\geq 54.36\%$.

5. Conclusions

In this work, the solubility of NIT in nine pure solvents and two kinds of binary mixtures at tested temperature range (278.15 K ~ 323.15 K) under atmospheric pressure ($p = 0.1$ MPa). In all the tested solvent systems, the solubility of NIT increases with the increasing temperature and the ratio of phenethylol/acetonitrile in binary solvents. The overall root mean square deviations (ORMSD) of the Van't Hoff model is lowest in both mono-solvents. The value of GSM model is lowest in ethanol + phenethylol and Van't-Hoff model is lowest in ethanol + acetonitrile. The results prove that the solubility of NIT in the tested solvent is the result of the combined effect of volume-dependent, solvent polarity and other factors.

Based on the apparent thermodynamic analysis, the thermodynamic properties for the solution process including enthalpy, entropy and Gibbs energy were calculated. According to the results, indicating that the dissolution process of NIT in all solvents is endothermic and not spontaneous. Through the above research will offer an assistance for design and optimization of crystallization and dosage form of NIT.

Declaration of Competing Interest

The authors declare that they have no known competing financial interests or personal relationships that could have appeared to influence the work reported in this paper.

Appendix A. Supplementary material

Supplementary data to this article can be found online at <https://doi.org/10.1016/j.arabj.2022.104531>.

References

- Akay, S., Kayan, B., Jouyban, A., Martínez, F., 2021. Solubility and dissolution thermodynamics of 5-fluorouracil in (ethanol + water) mixtures. *J. Mol. Liq.* 333,. <https://doi.org/10.1016/j.molliq.2021.116038> 116038.
- Alanazi, A., Alshehri, S., Altamimi, M., Shakeel, F., 2020. Solubility determination and three dimensional Hansen solubility parameters of gefitinib in different organic solvents: Experimental and computational approaches. *J. Mol. Liq.* 299,. <https://doi.org/10.1016/j.molliq.2019.112211> 112211.
- Alshehri, S., Shakeel, F., 2020. Solubility determination, various solubility parameters and solution thermodynamics of sunitinib malate in some cosolvents, water and various (Transcutol + water) mixtures. *J. Mol. Liq.* 307,. <https://doi.org/10.1016/j.molliq.2020.112970> 112970.
- Asadi, P., Kodide, K., Kota, M., Thati, J., 2020. Determination and correlation of solubility and solution thermodynamics of 4-aminobenzenesulfonamide in five binary solvent mixtures from 278.15 to 318.15 K. *J. Mol. Liq.* 303,. <https://doi.org/10.1016/j.molliq.2020.112670> 112670.
- Azarmi, S., Roa, W., Löbenberg, R., 2007. Current perspectives in dissolution testing of conventional and novel dosage forms. *Int. J. Pharm.* 328, 12–21. <https://doi.org/10.1016/j.ijpharm.2006.10.001>.
- Brett, H., 2007. Opening the Gateway: St. Louis Union Station. *Civ. Eng. Mag.* 77, 32–33. <https://doi.org/10.1061/ciegag.0000795>.
- Cao, Z., Zhang, R., Hu, X., Sha, J., Jiang, G., Li, Y., Li, T., Ren, B., 2020. Thermodynamic modelling, Hansen solubility parameter and solvent effect of oxaprozin in thirteen pure solvents at different temperatures. *J. Chem. Thermodyn.* 151,. <https://doi.org/10.1016/j.jct.2020.106239> 106239.
- Chen, S., Liu, Q., Dou, H., Zhang, L., Pei, L., Huang, R., Shu, G., Yuan, Z., Lin, J., Zhang, W., Peng, G., Zhong, Z., Yin, L., Zhao, L., Fu, H., 2020. Solubility and dissolution thermodynamic properties of Mequindox in binary solvent mixtures. *J. Mol. Liq.* 303. <https://doi.org/10.1016/j.molliq.2020.112619>.
- Corbett, J.R., Goose, J., 1971. A possible biochemical mode of action of the fasciolicides nitroxylin, hexachlorophene and oxyclozanide. *Pestic. Sci.* 2, 119–121. <https://doi.org/10.1002/ps.2780020307>.
- Greenhalgh, D.J., Williams, A.C., Timmins, P., York, P., 1999. Solubility parameters as predictors of miscibility in solid dispersions. *J. Pharm. Sci.* 88, 1182–1190. <https://doi.org/10.1021/js9900856>.
- Huang, W., Wang, H., Li, C., Wen, T., Xu, J., Ouyang, J., Zhang, C., 2021. Measurement and correlation of solubility, Hansen solubility parameters and thermodynamic behavior of Clozapine in eleven mono-solvents. *J. Mol. Liq.* 333,. <https://doi.org/10.1016/j.molliq.2021.115894> 115894.
- Jia, Q., Lei, D., Zhang, S., Zhang, J., Liu, N., Kou, K., 2021. Solubility measurement and correlation for HNIW-TNT co-crystal in nine pure solvents from T = (283.15 to 318.15) K. *J. Mol. Liq.* 323,. <https://doi.org/10.1016/j.molliq.2020.114592> 114592.
- Jouyban, K., Mazaher Haji Agha, E., Hemmati, S., Martínez, F., Kuentz, M., Jouyban, A., 2020. Solubility of 5-aminosalicylic acid in N-methyl-2-pyrrolidone + water mixtures at various temperatures. *J. Mol. Liq.* 310, 113143. <https://doi.org/https://doi.org/10.1016/j.molliq.2020.113143>
- Li, X., Cheng, C., Cong, Y., Du, C., Zhao, H., 2017. Determination and modelling of solid-liquid phase equilibrium and phase diagram for multicomponent system of nitrobenzaldehyde isomers. (I) Ternary system of 4-nitrobenzaldehyde + 3-nitrobenzaldehyde + ethyl acetate. *J. Mol. Liq.* 234, 164–171. <https://doi.org/10.1016/j.molliq.2017.03.044>.
- Li, C., Wang, H., Huang, W., Wen, T., Xu, J., Ouyang, J., Zhang, C., 2021. Solubility measurement, modeling and Hansen solubility parameters of 8-Chloro-11-(4-methyl-1-piperazinyl)-5H-dibenzo[b, e][1,4]diazepine in four binary solvents. *J. Mol. Liq.* 339,. <https://doi.org/10.1016/j.molliq.2021.116733> 116733.
- Liu, Y., Guo, H., 2021. Solubility determination and crystallization thermodynamics of an intermediate in different organic solvents. *J. Mol. Liq.* 339,. <https://doi.org/10.1016/j.molliq.2021.116821> 116821.
- Liu, Q., Yan, Y., Wu, Y., Zhang, X., Zhou, X., 2021. Systematic thermodynamic study of clorsulon dissolved in ten organic solvents: Mechanism evaluation by modeling and molecular dynamic simulation. *J. Mol. Liq.* 341,. <https://doi.org/10.1016/j.molliq.2021.117217> 117217.
- Mohammad, M.A., Alhalaweh, A., Velaga, S.P., 2011. Hansen solubility parameter as a tool to predict cocrystal formation. *Int. J. Pharm.* 407, 63–71. <https://doi.org/10.1016/j.ijpharm.2011.01.030>.
- Osorio, I.P., Martínez, F., Delgado, D.R., Jouyban, A., Acree, W.E., 2020. Solubility of sulfacetamide in aqueous propylene glycol mixtures: Measurement, correlation, dissolution thermodynamics, preferential solvation and solute volumetric contribution at saturation. *J. Mol. Liq.* 297,. <https://doi.org/10.1016/j.molliq.2019.111889> 111889.
- Rezaei, H., Rezaei, H., Rahimpour, E., Martínez, F., Jouyban, A., 2021. Solubility profile of phenytoin in the mixture of 1-propanol and water at different temperatures. *J. Mol. Liq.* 334,. <https://doi.org/10.1016/j.molliq.2021.115936> 115936.
- Sha, J., Hu, K., Li, T., Cao, Z., Wan, Y., Sun, R., He, H., Jiang, G., Li, Y., Li, T., Ren, B., 2021a. Solubility determination, model correlation, solvent effect, molecular simulation and thermodynamic properties of flutamide in eleven pure solvents at different temperatures. *J. Mol. Liq.* 336. <https://doi.org/10.1016/j.molliq.2021.115559>.

- Shekaari, H., Zafarani-Moattar, M.T., Shayanfar, A., Mokhtarpour, M., 2018. Effect of choline chloride/ethylene glycol or glycerol as deep eutectic solvents on the solubility and thermodynamic properties of acetaminophen. *J. Mol. Liq.* 249, 1222–1235. <https://doi.org/10.1016/j.molliq.2017.11.057>.
- Shen, F., Zhang, T., Li, Y., 2021. Determination and correlation of solubility of an explosive in different pure solvents. *J. Mol. Liq.* 340,. <https://doi.org/10.1016/j.molliq.2021.117169> 117169.
- Soliman, M., Saad, A.S., Ismail, N.S., Zaazaa, H.E., 2021. A validated RP-HPLC method for determination of nitroxynil and investigation of its intrinsic stability. *J. Iran. Chem. Soc.* 18, 351–361. <https://doi.org/10.1007/s13738-020-02030-w>.
- Sun, W., Shen, W., Xu, H., Hu, G., Deng, Z., Zhao, G., Li, F., Hu, Y., Yang, W., 2021. Determination and analysis of flutamide solubility in different solvent systems at different temperatures ($T = 278.15$ – 323.15 K). *J. Mol. Liq.* 325,. <https://doi.org/10.1016/j.molliq.2020.114762> 114762.
- Sun, R., Wen, Y., He, H., Yuan, L., Wan, Y., Sha, J., Dong, J., Li, Y., Li, T., Ren, B., 2021. Uridine in twelve pure solvents: Equilibrium solubility, thermodynamic analysis and molecular simulation. *J. Mol. Liq.* 330,. <https://doi.org/10.1016/j.molliq.2021.115663> 115663.
- Wei, J., Chen, S., Fu, H., Wang, X., Li, H., Lin, J., Xu, F., He, C., Liang, X., Tang, H., Shu, G., Zhang, W., 2021. Measurement and correlation of solubility data for atorvastatin calcium in pure and binary solvent systems from 293.15 K to 328.15 K. *J. Mol. Liq.* 324. <https://doi.org/10.1016/j.molliq.2020.115124>.
- Xue, M., Huang, D., Yang, K., Chen, L., Zheng, Z., Xiang, Y., Huang, Q., Wang, J., 2021. Measurement, correlation of solubility and thermodynamic properties analysis of 2,4,6-trinitroresorcinol hydrate in pure and binary solvents. *J. Mol. Liq.* 330,. <https://doi.org/10.1016/j.molliq.2021.115639> 115639.
- Yang, W.-Z., Fan, G.-Q., Zhang, T.-T., Li, D.-B., Pei, L.-L., Huang, R.-Y., Yin, D.-P., Zhang, L., Peng, G.-N., Shu, G., Yuan, Z.-X., Lin, J.-C., Zhang, W., Zhong, Z.-J., Yin, L.-Z., Fu, H.-L., 2021. Determination of the solubility and thermodynamic properties of albendazole in a binary solvent of ethanol and water. *Phys. Chem. Liq.* 59. <https://doi.org/10.1080/00319104.2019.1660979>.
- Yang, Z., Shao, D., Zhou, G., 2019. Solubility parameter of lenalidomide for predicting the type of solubility profile and application of thermodynamic model. *J. Chem. Thermodyn.* 132, 268–275. <https://doi.org/10.1016/j.jct.2018.12.035>.
- Zhang, C., Jouyban, A., Zhao, H., Farajtabar, A., Acree, W.E., 2021. Equilibrium solubility, Hansen solubility parameter, dissolution thermodynamics, transfer property and preferential solvation of zonisamide in aqueous binary mixtures of ethanol, acetonitrile, isopropanol and N, N-dimethylformamide. *J. Mol. Liq.* 326,. <https://doi.org/10.1016/j.molliq.2020.115219> 115219.